Taylor & Francis
Taylor & Francis Group

Liquid-crystalline pillar[5]arene-based [2]rotaxanes

Pauline Pieper[a], Yassine Chadi[a], Iwona Nierengarten [b], Uwe Hahn [b], Eric Meichsner [b], Thi Le Anh Nguyen [c,d], Joaquín Barberá [e], Robert Deschenaux [a] and Jean-François Nierengarten [b]

[a]Institut de Chimie, Université de Neuchâtel, Neuchâtel, Switzerland; [b]Laboratoire de Chimie des Matériaux Moléculaires, Ecole Européenne de Chimie, Polymères et Matériaux, Université de Strasbourg et CNRS (LIMA - UMR 7042), Strasbourg, France; [c]Institute of Research and Development, Duy Tan University, Da Nang, Vietnam; [d]Faculty of Natural Sciences, Duy Tan University, Da Nang, Vietnam; [e]Departamento de Química Orgánica, Instituto de Nanociencia y Materiales de Aragón, Universidad de Zaragoza – CSIC, Zaragoza, Spain

ABSTRACT

Liquid-crystalline mechanically interlocked molecules have been prepared from a clickable pillar[5] arene-containing [2]rotaxane building block incorporating ethynylated stoppers and dendritic mesogenic subunits of generation 0, 1 and 2 under copper-catalysed alkyne-azide cycloaddition conditions. The liquid-crystalline properties of the resulting pillar[5]arene-based rotaxanes bearing 4, 8 and 16 peripheral cyanobiphenyl units have been investigated and compared to those of corresponding model compounds lacking the macrocyclic component.
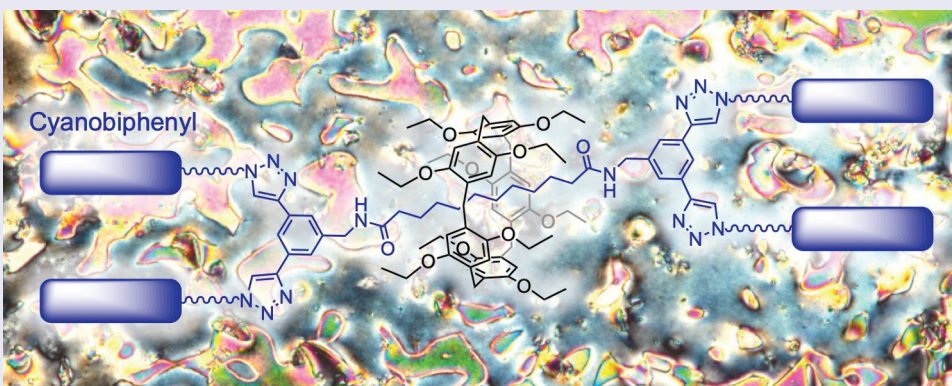
Introduction

Pillar[5]arenes are fascinating tubular-shaped macrocyclic compounds with two identical rims bearing both five alkyloxy substituents [1]. Following their discovery in 2008 [2], they became rapidly important building blocks in the field of supramolecular chemistry owing to their easy preparation [1]. On the other hand, the presence of their ten peripheral substituents makes pillar[5]arenes attractive compact scaffolds for the design of multifunctional nanomaterials [3]. The most efficient strategy for the preparation of such compounds is based on the ten-fold post-functionalization of easily affordable pillar[5]arene building blocks. The copper-catalysed alkyne-azide cycloaddition (CuAAC) reaction [4] is a particularly efficient synthetic tool for such a purpose [5]. The post-functionalization of pillar[5] arene building blocks bearing ten peripheral terminal alkyne or azide functions gave effectively access to a large variety of nanomaterials for various applications in materials science [6–10] or biology [11–16]. This strategy has been used, for example, to generate liquid-crystalline (LC) pillar[5]arene derivatives [17–23]. The first example has been obtained by grafting ten peripheral cyanobiphenyl mesogenic moieties onto the pillar [5]arene scaffold [17]. Comparison of the LC properties of this cyclopentamer with those of a corresponding

model monomer revealed the strong influence of the macrocyclic structure. Whereas a broad enantiotropic smectic A phase has been observed for the pillar[5]arene derivative, only a monotropic mesophase has been evidenced for the corresponding monomeric compound. Indeed, the macrocyclic core unit decreases the crystallinity of the material by preventing intermolecular π-π interactions between hydroquinone moieties as observed in the case of the monomer. On the other hand, the macrocyclic structure also provides orientational and/or positional disorder within the smectic layers while forcing, at the same time, the mesogenic units to adopt a supramolecular organisation in which each neighbouring smectic layer is interdigitated with its neighbours. As a result, the mesophase is stabilised by intermolecular interactions between the cyanobiphenyl subunits and is therefore stable over a broad temperature range. Similar observation have been recently reported by Ogoshi for pillar[5]arene derivatives substituted with peripheral mesogenic azobenzene subunits [22]. In this particular case, a lamellar organisation has been evidenced for the cyclopentamer but no liquid-crystalline properties could be observed for the corresponding model monomer. This additional example further highlights the essential role played by the macrocyclic structure for the stabilisation of mesophases. Finally, grafting Percec-type poly(benzyl ether) dendrons onto the pillar[5]arene scaffold generated disc-shaped molecules that self-organised into columnar wires with hexagonal Col_h columnar symmetry [20]. As part of this research, we became interested in a new design principle for the preparation of liquid-crystalline pillar[5]arene-containing LC materials. Specifically, mesomorphic dendrimers acting as strong self-organisation promoters have been grafted onto the axle component of a pillar[5]arene-based [2]rotaxane (Figure 1). The mesogenic moieties are therefore mechanically linked to the pillar[5]arene subunit but not covalently. In order to evaluate the influence of the pillar[5]arene moiety on the mesomorphic properties of rotaxanes **1a-c**, the corresponding compounds lacking the macrocycle were also prepared (**2a-c**). While a few examples of liquid-crystalline [2]rotaxanes have been already reported [24–29], compounds **1a-c** represent the first examples of pillar[5]arene-containing derivatives with mesomorphic properties.

Experimental section

General

Reagents were purchased as reagent grade and used without further purification. Compounds **3a-c** [30], **4**

[31] and **12** [32] were prepared according to a previously reported procedure. Acetonitrile (CH_3CN) and dichloromethane (CH_2Cl_2) were distilled over CaH_2 under Ar. All reactions were performed in standard glassware under an inert Ar atmosphere. Evaporation and concentration were done at water aspirator pressure and drying in vacuo at 10^{-2} Torr. Column chromatography: silica gel 60 (230–400 mesh, 0.040–0.063 mm) was purchased from E. Merck. Thin Layer Chromatography (TLC) was performed on aluminium sheets coated with silica gel 60 F_{254} purchased from E. Merck. NMR spectra were recorded with a Bruker AC 300 and AC 400 spectrometer with solvent peaks as reference. The ^1H signals were assigned by 2D experiments (COSY and NOESY). IR spectra (cm^{-1}) were recorded with a Perkin – Elmer Spectrum One spectrophotometer. MALDI-TOF and ESI-TOF mass spectra were recorded by the analytical service of the School of Chemistry (Strasbourg, France) and the University of Fribourg (Switzerland). Elemental analyses were performed by the service of the Fédération de Chimie Le Bel (Strasbourg, France) and Mikroelementarisches Laboratorium, ETH (Zürich, Switzerland).

Liquid-crystalline properties

Transition temperatures and enthalpies were determined with a differential scanning Mettler-Toledo DSC1 STARe System at a rate of 10°C/min, under N_2. Optical studies were made using a Zeiss-Axioskop polarising microscope equipped with a Linkam THMS-600 variable-temperature stage. XRD experiments were performed in a pinhole camera (Anton-Paar) operating with a point-focused Ni-filtered Cu-Kα beam. Lindemann glass capillaries with 0.9 mm diameter were used to contain the sample. When necessary, a variable-temperature oven was used to heat the sample. The capillary axis was placed perpendicular to the X-ray beam and the pattern was collected on flat photographic film perpendicular to the X-ray beam. Bragg's law was used to obtain the spacing.

General procedure for the preparation of liquid-crystalline rotaxanes 1a-c

A mixture of **13** (1 equiv.), azide **5a-c** (6–10 equiv.), copper catalyst (0.1–1 equiv.) and TBAF (4.8 equiv.) in CH_2Cl_2 (4 mL) or CH_2Cl_2/H_2O (1.5:1 mL) was stirred under Ar at room temperature for 24 h. The reaction was quenched with aq. NH_3 solution (2 M, 10 mL). The mixture was washed with an aq. NH_4Cl solution (10 mL) and extracted with CH_2Cl_2 (3 × 10 mL). The combined organic layer was dried ($MgSO_4$), filtered and
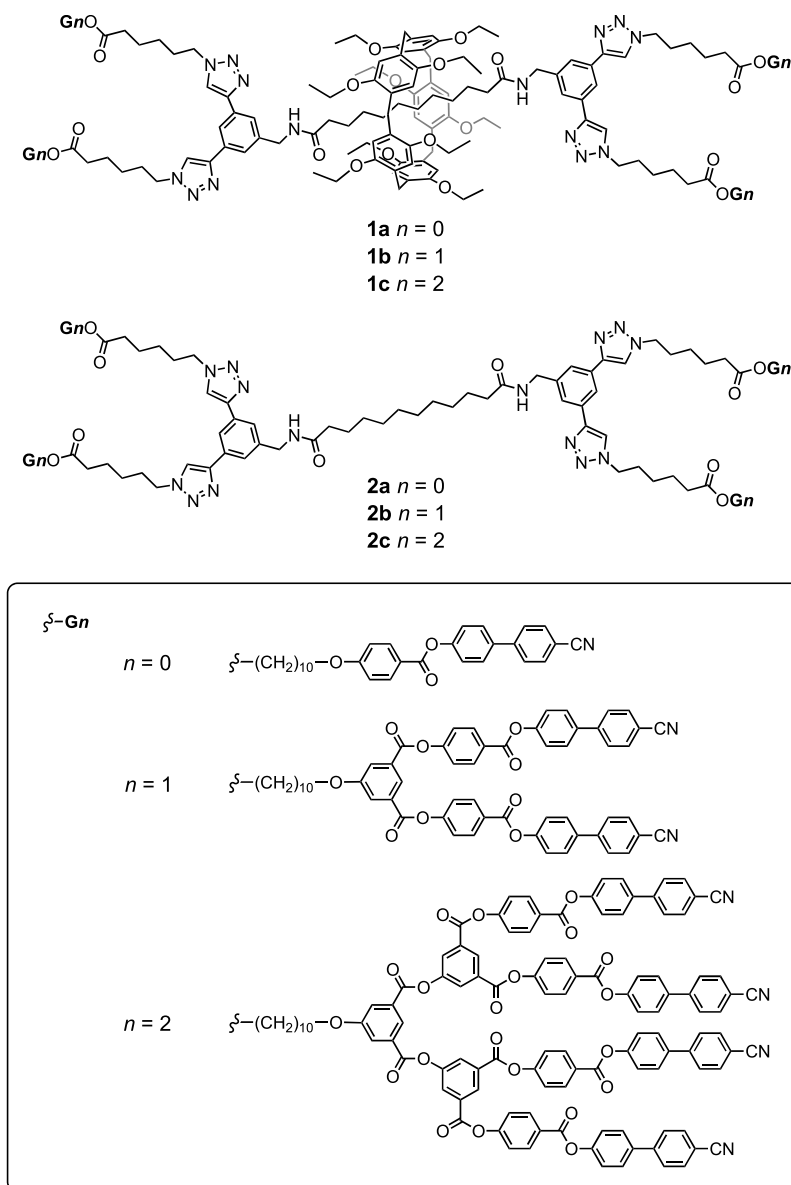
Figure 1. Structures of the liquid-crystalline pillar[5]arene-based [2]rotaxanes (**1a-c**) and their corresponding model compounds (**2a-c**).

concentrated. Purification by column chromatography (SiO₂, CH₂Cl₂ containing 2% of MeOH) followed by precipitation (dissolved in CH₂Cl₂ and precipitated dropwise into methanol) gave rotaxanes **1a-c**.

Compound 1a

From **13** (90 mg, 0.049 mmol), **5a** (180 mg, 0.293 mmol), [Cu(CH₃CN)₄]PF₆ (18.2 mg, 0.049 mmol) and TBAF (61.3 mg, 0.234 mmol) in CH₂Cl₂ (4 mL). Colourless liquid-crystalline product (37%, 70 mg). IR (neat): $v = 2225$ (C≡N), 1732 (COO), 1604 (CONH) cm⁻¹. GPC (dispersity): 1.01. ¹H NMR (400 MHz, CDCl₃): $\delta = 8.25$ (s, 2 H), 8.15 (d, $J = 8.1$ Hz, 8 H), 7.94 (s, 4 H), 7.74 (s, 4 H), 7.74 (d, $J = 7.8$ Hz, 8 H), 7.68 (d, $J = 7.8$ Hz, 8 H), 7.63 (d, $J = 7.6$ Hz, 8 H), 7.33 (d, $J = 7.6$ Hz, 8 H), 6.98 (d, $J = 8.1$ Hz, 8 H), 6.88 (s, 10 H), 6.36 (t, $J = 7$ Hz, 2 H), 4.62 (dd, $J = 14.6$ and 6.0 Hz, 2 H), 4.53 (dd, $J = 15.0$, 5.8 Hz, 2 H) 4.45 (t, $J = 6.9$ Hz, 8 H), 4.08 (m, 16 H), 3.95 (m, 10 H), 3.84 (m, 10 H), 3.72 (broad s, 10 H), 2.34 (t, $J = 7.4$ Hz, 8 H), 2.04 (m, 8 H), 1.85 (m, 8 H), 1.72 (m, 8 H), 1.62–1.31 (m, 98 H), 0.57 (broad s, 4 H), −0.08 (broad s, 4 H), −0.5 (broad s, 8 H) ppm. ¹³C NMR (100 MHz, CDCl₃): $\delta = 173.7, 173.5, 164.9, 163.8, 151.7, 149.8, 147.4, 145.0, 140.9, 136.8, 132.8, 132.5, 131.6, 128.6, 128.5, 127.8, 125.2, 122.7, 122.2, 121.4, 120.3, 119.0, 114.8, 114.5, 111.1, 68.5, 64.7, 63.9, 50.5, 43.4, 37.0, 34.1, 30.3, 30.2, 29.6$ (two peaks), 29.5, 29.4, 29.2, 28.9, 28.8, 28.7, 28.6, 26.2, 26.1, 26.0, 25.8, 24.4, 15.6 ppm. ESI⁺-TOF-MS: $m/z = 3861.05$ ([M+Na]⁺ calcd for C₂₃₃H₂₇₄N₁₈O₃₂Na: 3861.03). Anal. calcd for C₂₃₃H₂₇₄N₁₈O₃₂ (3838.80): C 72.90, H 7.19, N 6.57%; found: C 72.65, H 7.27, N 6.51%.

Compound 1b

From **13** (36.9 mg, 0.0199 mmol), **5b** (300.0 mg, 0.199 mmol), $CuSO_4 \cdot 5 H_2O$ (0.49 mg, 0.002 mmol), sodium ascorbate (2.36 mg, 0.012 mmol) and TBAF (24.97 mg, 0.096 mmol) in CH_2Cl_2/H_2O (1.5:1 mL). Colourless liquid-crystalline product (28%, 42 mg). IR (neat): $\nu =$ 3430 (CONH); 2226 (C≡N); 1729 (COO) cm^{-1}. GPC (dispersity): 1.01. ^{1}H NMR (400 MHz, $CDCl_3$): $\delta = 8.59$ (t, $J = 1.5$ Hz, 4 H), 8.23 (broad s, 2 H), 8.16–8.12 (m, 24 H), 8.06 (d, $J = 1.5$ Hz, 8 H), 7.91 (s, 4 H), 7.88 (d, $J = 1.5$ Hz, 4 H), 7.74 (d, $J = 8.6$ Hz, 16 H), 7.69 (d, $J = 8.6$ Hz, 16 H), 7.64 (d, $J = 8.6$ Hz, 16 H), 7.33 (d, $J = 8.6$ Hz, 16 H), 6.99–6.95 (m, 24 H), 6.88 (s, 10 H), 6.30 (t, $J = 5.9$ Hz, 2 H), 4.62–4.56 (m, 4 H), 4.45 (t, $J = 7.1$ Hz, 8 H), 4.36 (t, $J = 6.7$ Hz, 16 H), 4.07–4.01 (m, 32 H), 3.98–3.91 (m, 10 H), 3.87–3.80 (m, 10 H), 3.73 (broad s, 10 H), 2.34 (t, $J = 7.4$ Hz, 8 H), 2.03 (m, 8 H), 1.85–1.76 (m, 40 H), 1.72–1.66 (m, 8 H), 1.64–1.59 (m, 12 H), 1.45–1.30 (m, 182 H), 0.57 (broad s, 4 H), −0.07 (broad s, 4 H), −0.49 (broad s, 8 H) ppm. ^{13}C NMR (100 MHz, $CDCl_3$): $\delta = 173.6, 173.5, 165.2, 164.9, 164.7, 164.00, 163.8, 151.7, 151.2, 149.8, 147.2, 145.0, 140.2, 127.8, 127.45, 125.10, 122.70, 122.16, 121.34, 120.88, 120.19, 119.01, 114.8, 114.6, 114.5, 111.1, 68.5$ (two peaks), 65.9, 64.7, 63.9, 50.5, 43.5, 37.0, 34.1, 30.3, 30.2, 29.9, 29.6 (four peaks), 29.5 (two peaks), 29.4 (two peaks), 29.3, 29.2, 28.9, 28.8, 26.2 (two peaks), 26.1 (two peaks), 26.0, 25.9, 25.8, 24.4, 15.6 ppm. MALDI-TOF-MS: $m/z = 7437.68$ ([M+Na]$^+$ calcd for $C_{453}H_{510}N_{22}O_{72}Na$: 7438.08). Anal. calcd for $C_{453}H_{510}N_{22}O_{72}$ (7415.10): C 73.38, H 6.93, N 4.16%; found: C 73.12, H 6.98, N 3.99%.
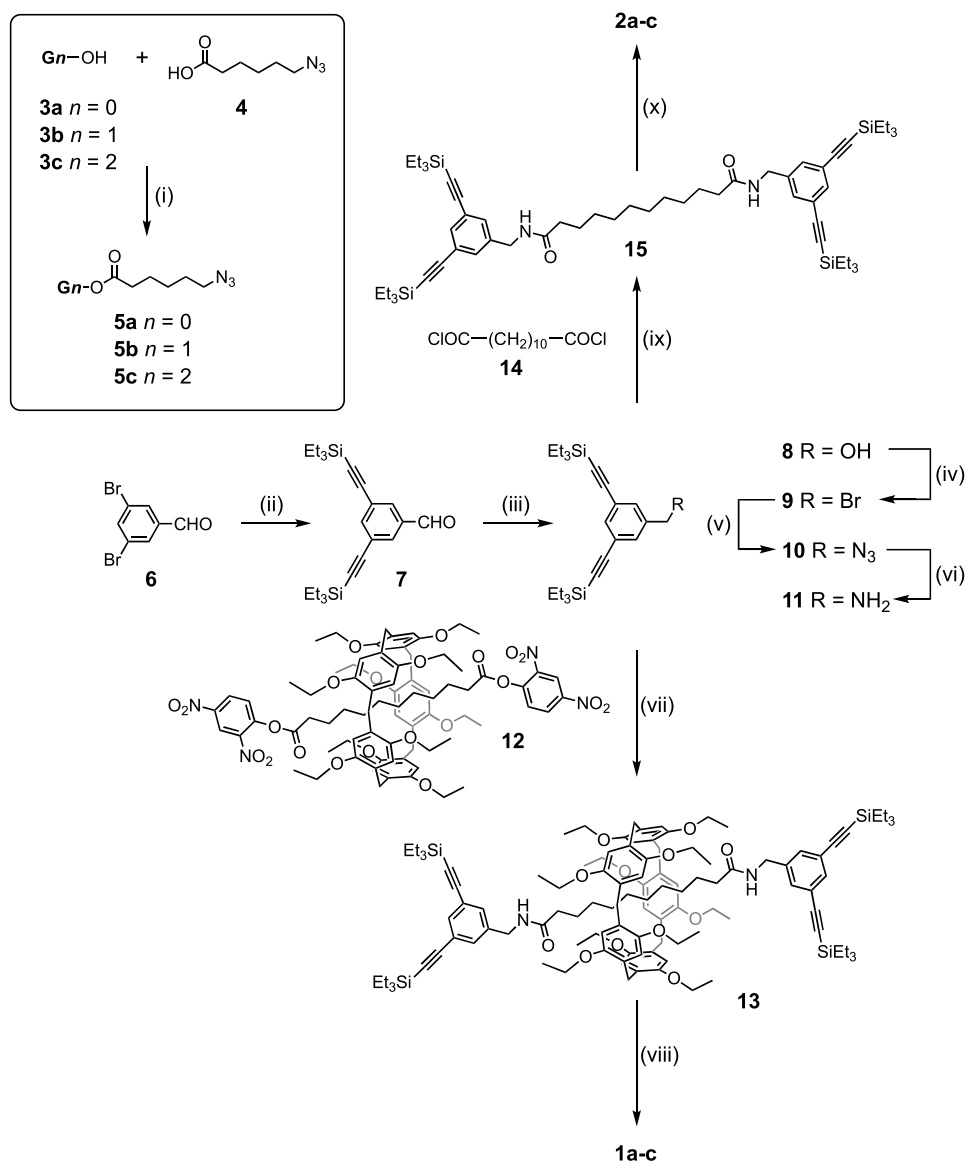
Compound 1c

From **13** (25.10 mg, 0.014 mmol), **5c** (300 mg, 0.109 mmol), $CuSO_4 \cdot 5 H_2O$ (0.33 mg, 0.001 mmol), sodium ascorbate (1.63 mg, 0.008 mmol) and TBAF (17.1 mg, 0.065 mmol) in CH_2Cl_2/H_2O (1.5:1 mL). Colourless liquid-crystalline product (27%, 45 mg). IR (neat): $\nu =$ 3435 (CONH); 2226 (C≡N); 1733 (COO) cm^{-1}. GPC (dispersity): 1.01. ^{1}H NMR (400 MHz, $CDCl_3$): $\delta = 8.93$ (broad s, 4 H), 8.63 (broad s, 8 H), 8.35 (broad s, 8 H), 8.20–8.10 (m, 58 H), 7.90 (s, 4 H), 7.86 (s, 4 H), 7.73 (d, $J = 8.2$ Hz, 32 H), 7.68 (d, $J = 8.4$ Hz, 32 H), 7.63 (d, $J = 8.5$ Hz, 32 H), 7.32 (d, $J = 8.5$ Hz, 32 H), 7.00–6.96 (m, 40 H), 6.87 (s, 10 H), 6.29 (t, $J = 5.4$ Hz, 2 H), 4.63–4.58 (m, 4 H), 4.44 (t, $J = 7.1$ Hz, 8 H), 4.36 (t, $J = 6.7$ Hz, 32 H), 4.07–4.01 (m, 48 H), 3.96–3.91 (m, 10 H), 3.86–3.80 (m, 10 H), 3.72 (broad s, 10 H), 2.33 (t, $J = 7.3$ Hz, 8 H), 2.03 (p, $J = 7.3$ Hz, 8 H), 1.89–1.80 (m, 72 H), 1.76–1.67 (m, 36 H), 1.51–1.35 (m, 262 H), 0.57 (broad s, 4 H), −0.07 (broad s, 4 H), −0.49 (broad s, 8 H) ppm. ^{13}C NMR (100 MHz, $CDCl_3$): $\delta = 173.5, 165.0, 164.9, 164.6, 164.2, 164.1, 163.8, 163.2, 151.8, 151.7, 150.7,$ 149.8, 147.3, 144.9, 136.8, 132.8, 132.7 (two peaks), 132.5, 131.2, 129.2, 128.7, 128.6, 128.5, 127.8 (two peaks), 127.1, 125.0, 122.7, 122.1, 121.3, 120.4, 120.1, 119.0, 114.8, 114.7, 114.5, 111.1, 68.6, 68.5, 66.0, 64.7, 63.9, 50.4, 43.5, 37.0, 34.1, 30.3, 30.2, 29.6 (five peaks), 29.5 (three peaks), 29.4 (three peaks), 29.3, 22.2, 29.2, 28.8, 26.2, 26.1 (three peaks), 26.0 (two peaks), 24.4, 15.6 ppm. MALDI-TOF-MS: $m/z = 12378.54$ ([M+Na]$^+$ calcd for $C_{757}H_{790}N_{30}O_{128}Na$: 12378.98). Anal. calcd for $C_{757}H_{790}N_{30}O_{128}$ (12357.00): C 73.58, H 6.44, N 3.40%; found: C 73.33, H 6.38, N 3.44%.

Results and discussion

Synthesis

The preparation of compounds **1a-c** and **2a-c** is depicted in Scheme 1. The synthetic approach to prepare those compounds relies on the functionalization of appropriate alkynylated precursors with azide building blocks equipped with peripheral cyanobiphenyl moieties under CuAAC conditions. Compounds **3a-c** [30] and **4** [31] were prepared as described in the literature. Reaction of alcohols **3a-c** with carboxylic acid **4** under esterification conditions using *N,N'*-dicyclohexylcarbodiimide (DCC) and 4-(dimethylamino)pyridinium *para*-toluenesulfonate (DPTS) [33] yielded the corresponding dendrons (**5a-c**) with an azide function at the focal point.

For the preparation of rotaxanes **1a-c**, a key precursor functionalised with alkyne functions was synthesised by taking advantage of the stopper exchange strategy recently developed by some of us for the efficient preparation of pillar[5]arene-based [2]rotaxanes [32,34,35]. For this purpose, the necessary amine reagent equipped with alkyne function was first prepared. Sonogashira cross-coupling reaction between commercially available 3,5-dibromobenzaldehyde (**6**) and triethylsilylacetylene gave aldehyde **7** (100%). Reduction of **7** with DIBAL-H led to alcohol **8** (87%). Bromination using CBr_4 and triphenylphosphine gave **9** which was converted into azide derivative **10** by treatment with sodium azide in *N,N*-dimethylformamide (DMF). Finally, reduction of azide **10** under Staudinger conditions afforded amine **11** (61%). Treatment of pillar[5]arene-containing rotaxane building block **12** bearing 2,4-dinitrophenol (DNP) ester stoppers [32] with an excess of amine **11** gave clickable rotaxane **13** in 93% yield. Importantly, the rotaxane structure is fully preserved during this chemical transformation. Indeed, this stopper exchange reaction occurs through an addition-elimination mechanism and unthreading of the axle moiety of the rotaxane is therefore prevented. Compound **13** was desilylated *in situ* with tetrabutylammonium fluoride

Scheme 1. Preparation of compounds **1a-c** and **2a-c** (for the structure of **G**n with n = 0, 1 or 2, see Figure 1). Reagents and conditions: (i) DPTS, DCC, CH₂Cl₂, rt (**5a**: 90%; **5b**: 74%; **5c**: 85%); (ii) Et₃SiCCH, [Pd(PPh₃)₂]Cl₂, CuI, PPh₃, Et₃N, THF, 80°C (100%); (iii) DIBAL-H, CH₂Cl₂, 0°C (87%); (iv) CBr₄, PPh₃, THF, 0°C → rt (100%); (v) NaN₃, DMF, rt (96%); (vi) PPh₃, THF/H₂O, rt (61%); (vii) Et₃N, CHCl₃, rt (93%); (viii) **5a-c**, Cu[(CH₃CN)₄]PF₆ with **5a** and CuSO₄·5 H₂O/sodium ascorbate/H₂O with **5b-c**, TBAF, CH₂Cl₂, rt, (**1a**: 37%, **1b**: 28%, **1c**: 27%); (ix) Et₃N, CH₂Cl₂ (83%); (x) **5a-c**, CuSO₄·5 H₂O, sodium ascorbate, TBAF, CH₂Cl₂/H₂O (1:1.5), rt (**2a**: 67%, **2b**: 52%, **2c**: 63%).

(TBAF) to generate the corresponding rotaxane intermediate bearing four terminal alkyne functions, to which azide dendrons **5a-c** were subsequently clicked. In a typical procedure, a mixture of [2]rotaxane **13** (1 equiv.), azide derivative **11** (6–10 equiv.) and the appropriate Cu(I)-catalyst in CH₂Cl₂ was stirred at room temperature for 20-24 h. Two copper catalysts were tested, i.e. Cu[(CH₃CN)₄]PF₆ and CuSO₄·5 H₂O/sodium ascorbate. For the synthesis of [2]rotaxane **1a**, the highest yield (37%) was obtained with Cu[(CH₃CN)₄]PF₆ in CH₂Cl₂. In contrast, optimal conditions for the *one-pot* synthesis of **1b** (28%) and **1c** (27%) were obtained with CuSO₄·5 H₂O (0.1 equiv.) and

sodium ascorbate (0.6 equiv.) in CH₂Cl₂/H₂O at room temperature. The moderate yields in pure **1a-c** can be explained by the difficulties encountered during their purification. In particular, traces of defected by-products with one or two unreacted terminal alkyne functions were difficult to remove and only a portion of pure final products could be isolated.

Finally, model compounds **2a-c** were prepared by a similar synthetic route. Treatment of dodecanedioyl dichloride (**14**) with an excess of amine **11** in the presence of Et₃N in CH₂Cl₂ gave compound **15**. Finally, reaction of **15** with **5a-c** in the presence of TBAF, CuSO₄·5 H₂O and sodium ascorbate in CH₂Cl₂/H₂O afforded **2a-c**.

The structure and purity of all the new compounds were confirmed by ^{1}H and ^{13}C NMR and IR spectroscopies, as well as by mass spectrometry and elemental analysis. As a typical example, the ^{1}H NMR spectra recorded in CDCl$_3$ at 25°C for compounds **1a** and **2a** are depicted in Figure 2. Comparison of the two spectra shows clearly the additional signals arising from the macrocyclic component of the rotaxane. Importantly, dramatic chemical shift changes are observed for some signals of the axle moiety in **1a** when compared to model compound **2a**. This is particularly the case for the resonances arising from the central -(CH$_2$)- chain located within the cavity of the macrocycle. The dramatic shielding observed for the resonances of H(1–5) in the rotaxane is actually due to the ring effect of the pillar[5]arene aromatic subunits on the methylene moieties of the axle. This is a characteristic spectroscopic signature observed for pillar[5]arene-containing rotaxanes [36–38] and this observation definitively supports the interlocked structure proposed for compound **1a**. Moreover, pairs of enantiotopic protons in axle **2a** are not any longer equivalent in rotaxane **1a**. Owing to the planar chirality of the pillar[5]arene macrocycle, such pairs of protons are actually diastereotopic in rotaxane **1a**. Chiral information transfer from the macrocycle to the axle is particularly clear for the signal of the benzylic methylene protons. Whereas a doublet was observed for the two equivalent benzylic protons H(6) in axle **2a**, a doublet of AB is detected for H(6/6') in rotaxane **1a**.

Liquid-crystalline properties

The phase-transition temperatures and enthalpies are reported in Table 1. The liquid-crystalline phases were identified by polarised optical microscopy from the observation of typical textures: focal-conic fan textures and homeotropic areas for the smectic A (SmA) phase, focal-conic fan and *schlieren* textures for the smectic C (SmC) phase and *schlieren* texture for the nematic (N) phase. Representative examples are shown in Figure 3.

Liquid-crystalline promoters **5a-c** gave rise to SmA and N phases. An additional SmC phase was observed for first-generation dendron **5b**. [2]Rotaxane **1a** developed a N phase. [2]Rotaxanes **1b-c** and dumbbells **2a-c** displayed smectic phases inherited from their dendritic moieties. The pillar[5]arene framework plays a significant role on the thermal stability of the mesophases. Indeed, the clearing temperatures displayed by the [2]rotaxanes are always lower than the ones of their corresponding model compounds. This effect is particularly important for derivatives **1a** and **2a** ($\Delta T = 64°C$), *i.e.*, the materials carrying the smallest number of mesogenic units. Moreover, liquid-crystalline promoters

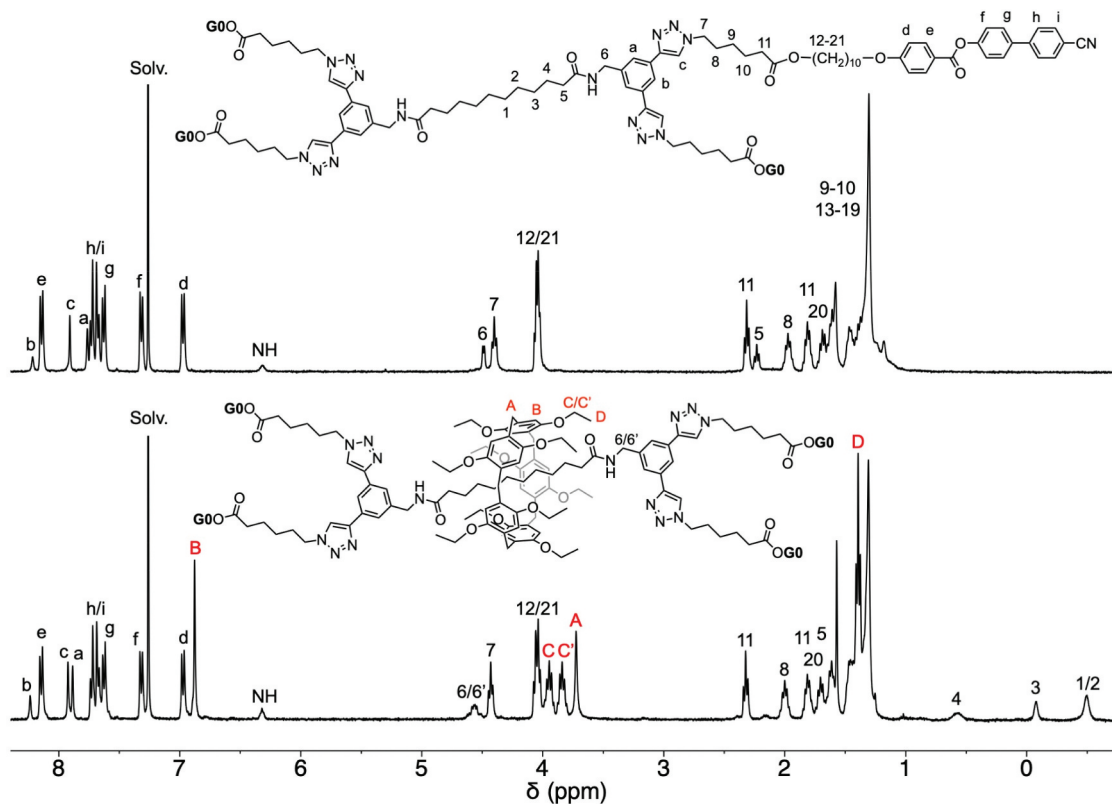**Figure 2.** (Colour online) ^{1}H NMR spectra (400 MHz) of compounds **1a** and **2a** recorded in CDCl$_3$ at 25°C.

Table 1. Phase transition temperatures and enthalpy changes of [2]rotaxanes **1a-c**, model compounds **2a-c** and liquid-crystalline promoters **5a-c**.[a]

Compound	Transitions	T/°C	ΔH/kJ·mol^{-1}
1a	N → I	99	_[b]
1b	SmC → SmA	95	_[c]
	SmA → I	152	27.5
1c	SmA → I	173	32.0
2a	SmA → I	163	9.0
2b	SmC → SmA	123	_[c]
	SmA → I	174	33.0
2c	SmA → I	187	39.0
5a	Cr → SmA	82	54.1
	SmA → N	147	0.6
	N → I	150	0.3
5b	SmC → SmA	72	_[c]
	SmA → N	148	0.2
	N → I	160	1.9
5c	SmA → N	175	9.5[d]
	N → I	176	

[a]Cr: crystalline or semi-crystalline solid; SmA: smectic A phase; SmC: smectic C phase; N: nematic phase; I: isotropic liquid. Transition temperatures are given as the onset of the peaks obtained during the second heating run. The T_g values could not be determined. [b]Negligible value. [c]Observed by polarised optical microscopy. [d]Combined enthalpies.

5-c displayed clearing temperatures which fall between those of the model compounds and the rotaxanes. This result can be explained by the fact that for model compounds **2a-c**, hydrogen bonds (*via* the amide functions) and π-π interactions (through the aromatic and triazole rings) are capable of providing an extra-stabilisation of the liquid-crystalline state. Such interactions are significantly weaker if not totally vanished in the case of [2]rotaxanes **1a-c** due to the presence of the pillar[5] arene subunit that prevents close interactions between the axle subunits of neighbouring molecules. Finally, the formation of nematic and smectic phases for **1a-c** and **2a-c** is fully consistent with the nature and structure of the cyanobiphenyl-based mesogens which tend to organise into layered structures [18,19,30].

Supramolecular organization

X-ray measurements (Table 2) confirmed the results obtained by optical microscopy and DSC. The diffractograms of **1a** gave only diffuse scattering at small and large angles, as expected for a nematic phase. Compound **1b** produced a typical diffractogram of a smectic phase. The measured layer spacing at room temperature is 97 Å. Compound **1c** also produced diffractograms typical of a smectic phase with two reflections observed in a reciprocal spacing ratio of 1:2. The spacing measured from these reflections is 53.5 Å, a much smaller value than expected for the size of the molecules and significantly smaller than the measured spacing for **1b**. It is so evident that the first observed maximum cannot correspond to first order reflection, and therefore the layer thickness is, in fact, twice the observed value (*i.e.*, 107 Å). This is consistent with the
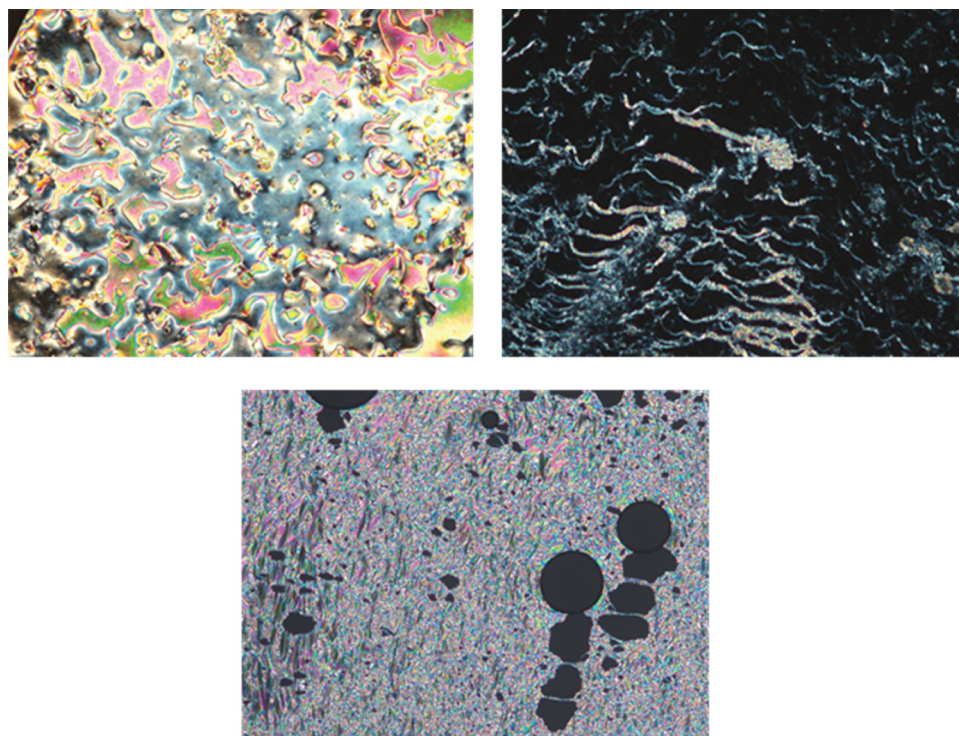

Figure 3. (Colour online) Thermal-polarised optical micrographs of (a) the *schlieren* texture displayed by **1a** in the N phase at 96°C (top left), (b) the focal-conic fan textures and homeotropic areas displayed by **1b** in the SmA phase at 120°C (top right), and (c) the focal-conic fan textures displayed by **1c** in the SmA phase at 168°C (bottom).

Table 2. Structural characterisation of the mesophases[.a].

Compound	T/°C	Phase	d_{obs}/Å	d_{layer}/Å
1a	rt	N	[b]	
1b	rt	SmC	97	97
	80	SmC	[b]	–
1c	rt	SmA	53.5 ; 26.7	107
2a	rt	SmA	72 ; 24	72
2b	rt	SmC	84	84
	60, 90 and 110	SmC	[b]	–
2c	rt	SmA	53 ; 26.5	106
	120	SmA	24.5	98
	170	SmA	24	96
5a	rt	Cr	–	–
	100	SmA	52.0	52.0
	145	SmA	51.5	51.5
5b	rt	Cr	–	–
	90	SmA	85.0	85.0
	120 and 145	SmA	82.0	82.0
5c	rt	SmA	56	112
	90	SmA	27	108

[a]Cr: crystalline or semi-crystalline state; SmA: smectic A phase; SmC: smectic C phase; N: nematic phase; I: isotropic liquid, rt: room temperature, d_{obs}: measured spacing, d_{layer} spacing of the layer of the smectic phase. [b]No reflection observed.

expected evolution from the previous generation. The thickness of the smectic layer for **1b** and **1c** is much shorter than the length of the molecule in the fully extended conformation and this reveals the conformational disorder of the hydrocarbon spacers as well as a high degree of interdigitation of the mesogenic units. This result is consistent with the effective decreased layer thickness previously reported for cyanobiphenyl functionalised pillar[n]arenes ($n = 5, 6$) [18]. The postulated supramolecular organisation of **1a-c** within the different mesophases is schematically represented in Figure 4.

Mesogenic promoters **5a-c** produced diffractograms characteristic of smectic phases. Although some reflections are absent, from the measured spacing it can be deduced that the thickness of the smectic layer of **5a-c** is respectively 52, 85 and 108 Å at 90–100°C. From the evolution of the layer spacing from 52 Å (for **5a**) to 85 Å (for **5b**), it can be deduced that the molecules of **5b** are packed in two sublayers. The molecular length (L) of the dendrons **5a-c** in their extended conformations was estimated by Hyperchem, and found to be 38, 63 and 78 Å for **5a**, **5b** and **5c**, respectively. Therefore, a d_{layer}/L ratio of 1.35–1.43 was found for **5a-c**. These values suggest that the mesogens are highly interdigitated. In each sublayer, the mesogenic units are
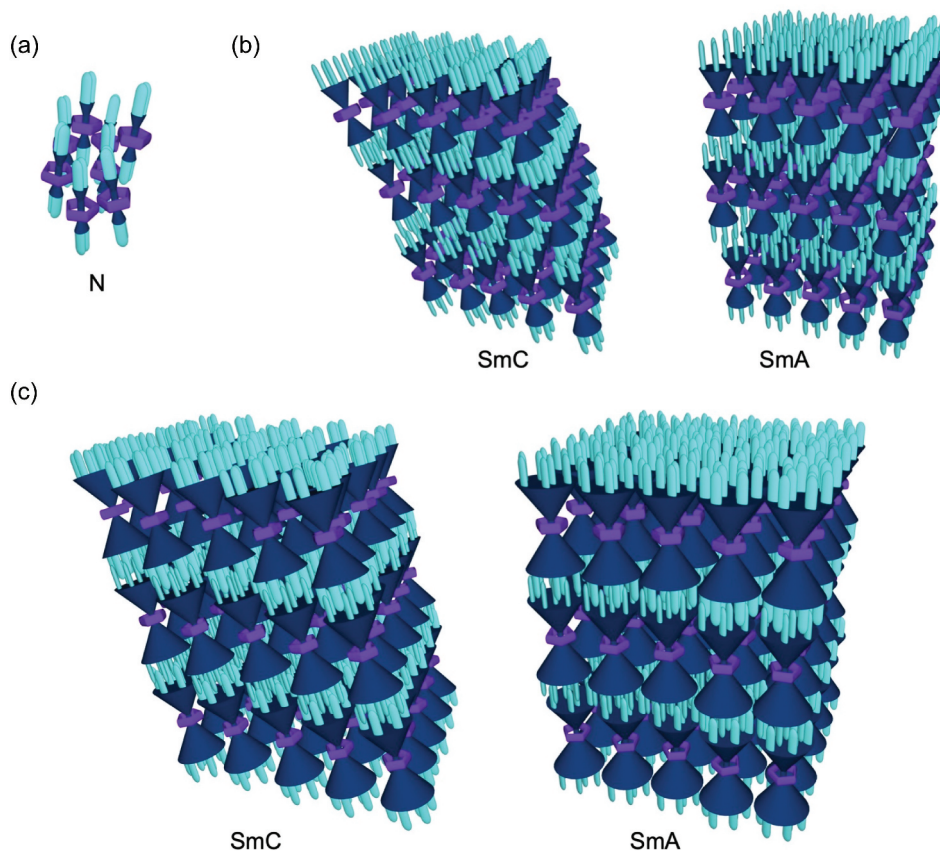

Figure 4. (Colour online) Postulated models of the supramolecular organisation of **1a** within the N phase (a); **1b** within the SmC and SmA phases (b), and **1c** within the SmC and SmA phases (c). Color code: pale blue tubes for the peripheral cyanobiphenyl units; dark blue for the inner part of the dendrons and the axle; purple for the pillar[5]arene.

oriented outward while the azide-terminated spacers are oriented inward with a high degree of interpenetration with the spacers of the other sublayer. The same structural model can be suggested for **5c**, where the interlayer spacing is greater than for **5b** as a consequence of the increased length of the molecule. In other words, for dendrons **5b** and **5c** three distinct regions can be distinguished within the smectic layers: a central slab containing the flexible spacer terminated by the azide group and two peripheral regions containing the mesogenic units pointing upward and downward with a significant degree of interdigitation in both regions.

For dumbbell-shaped model compounds **2a-c**, diffraction patterns typical of smectic phases were also observed. Some reflections are absent, as for the other compounds. The thickness of the smectic layer is 72, 84, and 106 Å at room temperature for **2a**, **2b** and **2c**, respectively.

Regarding the absence of some main reflections and the presence of high-order reflections, this phenomenon is not unexpected as a consequence of the peculiarities of the smectic packing of these compounds, in which differentiated regions can be distinguished and this segregation produces a complex periodicity in the projection of the electron density profile to the direction of the layer normal in addition to the main period [39–41]. In some cases, the high temperature patterns do not give any maximum, most likely, due to thermal degradation as a consequence of the long exposure times required for X-ray measurements.

Conclusions

A clickable [2]rotaxane building block incorporating an ethylated pillar[5]arene moiety and a symmetrical axle subunit bearing doubly ethynylated stoppers has been efficiently prepared by a stopper exchange strategy. Dendritic mesogenic subunits of generation 0, 1 and 2 have been grafted onto this supramolecular ensemble to generate liquid-crystalline pillar[5]arene-based rotaxanes bearing 4, 8 and 16 peripheral cyanobiphenyl mesogens. When compared to model compounds lacking the macrocyclic component, the presence of the pillar[5]arene moiety in the rotaxanes had a significant influence on the thermal stability of the mesophases by reducing the clearing temperature by about 20–60°C. For the smallest compounds bearing four cyanobiphenyl groups, steric effects resulting from the presence of the rather large pillar[5]arene moiety in rotaxane **1a** prevented the self-organisation into the lamellar mesophase observed for the corresponding model compound

(**2a**). In this case, only a nematic phase has been evidenced for the rotaxane. For the highest generation compounds (**1b-c** and **2b-c**), the mesogens are capable of promoting the same supramolecular organisation for both the rotaxanes and the model compounds. In other words, the high number of peripheral cyanobiphenyl groups is able to counterbalance steric effects resulting from the presence of the pillar[5]arene moiety in **1b-c**. In conclusion, we have shown that the proposed design principle is efficient for the preparation of pillar[5]arene-containing mesomorphic materials. This study therefore paves the way towards the preparation of new liquid-crystalline molecular machines with switchable properties. On the other hand, the preparation of analogous systems from optically pure pillar[5]arene-based rotaxane building blocks should provide unprecedented materials in which chirality transfer through mechanical bonds should influence the self-organisation into chiral mesophases. Work in this direction is underway in our laboratories.

Disclosure statement

No potential conflict of interest was reported by the author(s).

ORCID

Iwona Nierengarten ⓘ http://orcid.org/0000-0003-0501-6768
Uwe Hahn ⓘ http://orcid.org/0000-0003-3077-9361
Eric Meichsner ⓘ http://orcid.org/0000-0002-9193-2078
Thi Le Anh Nguyen ⓘ http://orcid.org/0000-0002-3660-8400
Joaquín Barberá ⓘ http://orcid.org/0000-0001-5816-7960
Robert Deschenaux ⓘ http://orcid.org/0000-0002-1142-0022
Jean-François Nierengarten ⓘ http://orcid.org/0000-0002-3333-9372

References

[1] Ogoshi T, Yamagishi TA, Nakamoto Y. Pillar-shaped macrocyclic hosts pillar[n]arenes: new key players for supramolecular chemistry. Chem Rev. 2016;116 (14):7937–8002. doi: 10.1021/acs.chemrev.5b00765

[2] Ogoshi T, Kanai S, Fujinami S, et al. *Para*-bridged symmetrical pillar[5]arenes: their Lewis acid catalyzed synthesis and host-guest properties. J Am Chem Soc. 2008;130(15):5022–5023. doi: 10.1021/ja711260m

[3] Nierengarten I, Holler M, Rémy M, et al. Grafting dendrons onto pillar[5]arene scaffolds. Molecules. 2021;26(8):2358. doi: 10.3390/molecules26082358

[4] Kolb HC, Finn MG, Sharpless KB. Click chemistry: diverse chemical function from a few good reactions. Angew Chem Int Ed. 2001;40(11):2004–2021. doi: 10.1002/1521-3773(20010601)40:11<2004:AID-ANIE2004>3.0.CO;2-5

[5] Kakuta T, Yamagishi T, Ogoshi T. Supramolecular chemistry of pillar[n]arenes functionalised by a copper-(I)-catalysed alkyne–azide cycloaddition "click" reaction. Chem Commun. 2017;53(38):5250–5266. doi: 10.1039/C7CC01833A

[6] Steffenhagen M, Latus A, Trinh TMN, et al. A rotaxane scaffold bearing multiple redox centers: synthesis, surface modification and electrochemical properties. Chem Eur J. 2018;24(7):1701–1708. doi: 10.1002/chem.201705245

[7] Bettucci O, Pascual J, Turren-Cruz S-H, et al. Dendritic-like molecules built on a pillar[5]arene core as hole transporting materials for perovskite solar cells. Chem Eur J. 2021;27(31):8110–8117. doi: 10.1002/chem.202101110

[8] Trinh TMN, Nierengarten I, Ben Aziza H, et al. Coordination-driven folding in multi-Zn(II)porphyrin arrays constructed on a pillar[5]arene scaffold. Chem Eur J. 2017;23(46):11011–11021. doi: 10.1002/chem.201701622

[9] Delavaux-Nicot B, Ben Aziza H, Nierengarten I, et al. A rotaxane scaffold for the construction of multiporphyrinic light-harvesting devices. Chem Eur J. 2018;24(1):133–140. doi: 10.1002/chem.201704124

[10] Dekhtiarenko M, Mengheres G, Levillain E, et al. Tetrathiafulvalene and π-extended tetrathiafulvalene pillar[5]arene conjugates: synthesis, electrochemistry and host-guest properties. New J Chem. 2023;47(16):7757–7764. doi: 10.1039/D3NJ01025B

[11] Nierengarten I, Buffet K, Holler M, et al. A mannosylated pillar[5]arene derivative: chiral information transfer and antiadhesive properties against uropathogenic bacteria. Tetrahedron Lett. 2013;54(19):2398–2402. doi: 10.1016/j.tetlet.2013.02.100

[12] Buffet K, Nierengarten I, Galanos N, et al. Pillar[5]arene-based glycoclusters: synthesis and multivalent binding to pathogenic bacterial lectins. Chem Eur J. 2016;22(9):2955–2963. doi: 10.1002/chem.201504921

[13] Vincent SP, Buffet K, Nierengarten I, et al. Biologically active heteroglycoclusters constructed on a pillar[5]arene-containing [2]rotaxane scaffold. Chem Eur J. 2016;22(1):88–92. doi: 10.1002/chem.201504110

[14] Galanos N, Gillon E, Imberty A, et al. Pentavalent pillar[5]arene-based glycoclusters and their multivalent binding to pathogenic bacterial lectins. Org Biomol Chem. 2016;14(13):3476–3481. doi: 10.1039/C6OB00220J

[15] Nierengarten I, Nothisen M, Sigwalt D, et al. Polycationic pillar[5]arene derivatives: interaction with DNA and biological applications. Chem Eur J. 2013;19(51):17552–17558. doi: 10.1002/chem.201303029

[16] Chang Y, Yang K, Wie P, et al. Cationic vesicles based on amphiphilic pillar[5]arene capped with Ferrocenium: a redox-responsive system for drug/siRNA co-delivery. Angew Chem Int Ed. 2014;24(48):13126–13130. doi: 10.1002/anie.201407272

[17] Nierengarten I, Guerra S, Holler M, et al. Building liquid crystals from the 5-fold symmetrical pillar[5]arene core. Chem Commun. 2012;48(65):8072–8074. doi: 10.1039/c2cc33746k

[18] Nierengarten I, Guerra S, Holler M, et al. Macrocyclic effects in the mesomorphic properties of liquid-crystalline pillar[5]- and pillar[6]arenes. Eur J Org Chem. 2013;2013(18):3675–3684. doi: 10.1002/ejoc.201300356

[19] Pan S, Ni M, Mu B, et al. Well-defined pillararene-based azobenzene liquid crystalline photo-responsive materials and their thin films with photo-modulated surfaces. Adv Funct Mater. 2015;25(23):3571–3580. doi: 10.1002/adfm.201500942

[20] Nierengarten I, Guerra S, Ben aziza H, et al. Piling up pillar[5]arenes to self-assemble nanotubes. Chem Eur J. 2016;22(18):6185–6189. doi: 10.1002/chem.201600688

[21] Concellon A, Romero P, Marcos M, et al. Coumarin-containing pillar[5]arenes as multifunctional liquid crystal macrocycles. J Org Chem. 2020;85(14):8944–8951. doi: 10.1021/acs.joc.0c00852

[22] Fa S, Mizobata M, Nagano S, et al. Reversible on/off chiral amplification of pillar[5]arene assemblies by dual external stimuli. ACS Nano. 2021;15(10):16794–16801. doi: 10.1021/acsnano.1c06975

[23] Chang Q, Zhao H, Ding W, et al. Facile synthesis of pillar[5]arene liquid crystals with formation of layer and tubular columnar phases. Phase Transitions. 2022;95(5):398–405. doi: 10.1080/01411594.2022.2046744

[24] Aprahamian I, Yasuda T, Ikeda T, et al. A liquid-crystalline bistable [2]rotaxane. Angew Chem Int Ed. 2007;46(25):4675–4679. doi: 10.1002/anie.200700305

[25] Baranoff ED, Voignier J, Yasuda T, et al. A liquid-crystalline [2]catenane and its copper(I) complex. Angew Chem Int Ed. 2007;46(25):4680–4683. doi: 10.1002/anie.200700308

[26] Kidowaki M, Nakajima T, Araki J, et al. Novel liquid crystalline polyrotaxane with movable mesogenic side chains. Macromolecules. 2007;40(19):6859–6862. doi: 10.1021/ma070785u

[27] Yasuda T, Tanabe K, Tsuji T, et al. A redox-switchable [2]rotaxane in a liquid-crystalline state. Chem Commun. 2010;46(8):1224–1226. doi: 10.1039/b922088g

[28] Sakuda J, Yasuda T, Kato T. Liquid-crystalline catenanes and rotaxanes. ISR J Chem. 2012;52(10):854–862. doi: 10.1002/ijch.201200045

[29] Suhan ND, Loeb SJ, Eichhorn SH. Mesomorphic [2]rotaxanes: sheltering ionic cores with interlocking components. J Am Chem Soc. 2013;135(1):400–408. doi: 10.1021/ja309558p

[30] Dardel B, Guillon D, Heinrich B, et al. Fullerene-containing liquid-crystalline dendrimers. J Mater Chem. 2001;11(11):2814–2831. doi: 10.1039/b103798f

[31] Chan-Seng D, Lutz J-F. Primary structure control of oligomers based on natural and synthetic building blocks. ACS Macro Lett. 2014;3(3):291–294. doi: 10.1021/mz5000575

[32] Nierengarten I, Meichsner E, Holler M, et al. Preparation of pillar[5]arene-based [2]rotaxanes by a stopper-exchange strategy. Chem Eur J. 2018;24 (1):169–177. doi: 10.1002/chem.201703997

[33] Moore JS, Stupp SI. Room temperature polyesterification. Macromolecules. 1990;23(1):65–70. doi: 10.1021/ma00203a013

[34] Nierengarten I, Nierengarten J-F. Diversity oriented preparation of pillar[5]arene-containing [2]rotaxanes by a stopper exchange strategy. ChemistryOpen. 2020;9(4):393–400. doi: 10.1002/open.202000035

[35] Rémy M, Nierengarten I, Park B, et al. Pentafluorophenyl esters as exchangeable stoppers for the construction of photoactive [2]rotaxanes. Chem Eur J. 2021;27 (33):8492–8499. doi: 10.1002/chem.202100943

[36] Trinh TMN, Nierengarten I, Holler M, et al. Langmuir and Langmuir-Blodgett films from amphiphilic pillar [5]arene-containing [2]rotaxanes. Chem Eur J. 2015;21 (22):8019–8022. doi: 10.1002/chem.201501124

[37] Milev R, Lopez-Pacheco A, Nierengarten I, et al. Preparation of pillar[5]arene-based [2]rotaxanes from acyl chlorides and amines. Eur J Org Chem. 2015;2015 (3):479–485. doi: 10.1002/ejoc.201403380

[38] Holler M, Stoerkler T, Louis A, et al. Mechanochemical solvent-free conditions for the synthesis of pillar[5]arene-containing [2]rotaxanes. Eur J Org Chem. 2019;2019 (21):3401–3405. doi: 10.1002/ejoc.201900153

[39] Zu X-Q, Liu J-H, Liu Y-X. Chen E-Q molecular packing and phase transitions of side chain liquid crystalline polymethacrylates based on p-methoxyazobenzene. Polymer. 2008;49:3103–3110. doi: 10.1016/j.polymer.2008.04.054

[40] Martinez-Felipe A, Lu Z, Henderson PA, et al. Synthesis and characterization of side-chain liquid crystalline copolymers containing sulfonic acid groups. Polymer. 2012;53:2604–2612. doi: 10.1016/j.polymer.2012.02.029

[41] Haege C, Jagiella S, Giesselmann F. Molecular electron density distribution and X-ray diffraction patterns of smectic a liquid crystals – a simulation study. Chemphyschem. 2019;20(19):2466–2472. doi: 10.1002/cphc.201900538